Collisional relaxation of selectively excited combination vibrational state (103) of the H_2O molecule

Yu.N. Ponomarev and O.Yu. Nikiforova

Institute of Atmospheric Optics,
Siberian Branch of the Russian Academy of Sciences, Tomsk

Received December 25, 2002

The literature experimental data on relaxation of (103) and (100–001) states of the H_2O molecule in pure water vapor and in its mixture with nitrogen and air are analyzed. Based on the model of the process of intramolecular energy exchange, we estimated relaxation rate constants for $(0V_20)$ band levels, as well as the mean energy transferred by the H_2O molecule collisionally excited to the (103) state. The mean collisional energy transferred is from 15–35 cm^{-1} (at excitation energy up to 3000–4000 cm^{-1}) to 100 cm^{-1} (at excitation energy of 14400 cm^{-1}).

Introduction

The information on the rates and ways of collisional deactivation of H_2O vibrational states at collisions with the main air constituents, N_2 and O_2, or their natural mixture is important for description of many processes with participation of molecules being in excited vibrational states (for example, processes connected with violation of the local thermodynamic equilibrium in the atmosphere, kinetics of medium heating at propagation of laser radiation) and for understanding of peculiarities in the energy exchange between colliding molecules. Theoretical description of the process of energy transfer between polyatomic molecules at binary collisions, especially, in the case of strong vibrational anharmonism is difficult even for the case of collision with atoms of inert gases.[1]

A theoretical model describing relaxation of a high-excited vibrational state in a strongly anharmonic and light molecule, such as H_2O, is extremely complicated.[2] In this connection, of great importance are experimental data on relaxation of various selectively excited high vibrational molecular energy levels and estimates of the basic relaxation channels.

For asymmetric-top triatomic molecules (O_3, H_2O, SO_2) it was shown that relaxation of energy levels corresponding to stretching vibrational modes of (V_100) and $(00V_3)$ type, where V_1 and V_3 are the vibrational quantum numbers, involves two stages.[3–9] First, intramolecular energy exchange occurs between the stretching mode and the closest bending mode, for example, $(V_100) \rightarrow (0V_20)$. For high H_2O vibrational levels, this exchange is favored by the fact that vibrational states are strongly mixed because of the large number of accidental resonances.[10] Then relaxation occurs at vibrational levels $(0V_20)$ of the bending mode (transitions $V_2 \rightarrow (V_2 - 1)$). The rates of these transitions increase with increasing V_2, and the duration of vibrational-translational relaxation is mostly determined by the time of vibrational-translational (VT) relaxation of the lowest state $V_2 = 1$.

In this paper, we have analyzed the results of previous experimental studies[3–5,11–13] of vibrational relaxation at laser excitation of the (103) and (100–001) states of H_2O molecule in pure water vapor and in its mixtures with nitrogen and air. As a result of this analysis, we have estimated the relaxation rate constants for the energy levels of the $(0V_20)$ band corresponding to the model of a harmonic oscillator, as well as the mean energy transferred by the H_2O molecule for one collision at its excitation up to the state (103) with the total vibration energy of 19000 cm^{-1}.

1. Experiment

Experimental studies of vibrational relaxation in H_2O, whose results are analyzed in this paper, were conducted by fluorescent[3–5] and photoacoustic[11–13] methods. The method of laser fluorescence is based on measuring the kinetics of radiation emitted by a molecule at its transition from an excited vibrational state to a lower-lying vibrational state. The steepness of the increase and decrease in the intensity of emitted radiation characterizes the population and relaxation rates of the studied (fluorescing) level. Observation of fluorescence at different wavelengths allows one to judge on the population and depopulation rates of different vibrational levels of the molecule and to determine the rate constants of some vibrational transitions. The photoacoustic (PA) method allows determination of the time of radiationless relaxation of the excited vibrational state,[14,15] that is, the time needed for molecules to transform the energy of the exciting radiation into heat at collisions.

There exist several versions of application of the PA method to determination of the VT relaxation time in gases at excitation of a certain vibrational state by a short laser pulse with duration $\tau_p \ll \tau_{VT}$ and analysis of kinetics of the signal generated in a PA cell, whose design provides for the space and time resolution of detected signals.[9,11–15] When using a periodically

modulated exciting radiation, one can obtain from the PA measurements an idea of the prevalent relaxation channel and determine the rate constants of the component transitions,[6,9] making it up, while at excitation with pulsed radiation there are some peculiarities in analysis of relaxation channels and such analysis was not performed (see Refs. 11–13).

Table 1 summarizes the results of experimental studies[3–5,11–13] of relaxation at excitation of the (100–001) and (103) vibrational states for both pure water vapor and the mixture of H_2O with air, nitrogen, and oxygen. Since the rates of individual relaxation processes were not obtained in Refs. 11–13, the results of Refs. 3–5 and Refs. 11–13 can hardly be compared directly. Therefore, for a convenience, the Table rows containing the relaxation rates from Refs. 3–5 give also the relaxation times corresponding to individual transitions and the total time of vibrational relaxation in a multilevel system that were calculated by us (for the H_2O pressure of 1 Torr) from the corresponding rate values by the equations:

$$\tau(V_1V_2V_3 \to V_1'V_2'V_3') = 1/k(V_1V_2V_3 \to V_1'V_2'V_3'),$$

$$\tau_\Sigma = \sum_i \frac{1}{k_i}.$$

The relaxation time for the (103) vibration was estimated in Refs. 11 and 12 from the dependence of the phase of free oscillation of a microphone membrane on the pressure of a gas in the PA cell under study. Though measurements were conducted in the pressure range, where the membrane inertia is not very significant, it still could lead to overestimated time as compared to the true one. Therefore, although the data from Refs. 11 and 12 are included in Table 1, in the further analysis we used the results of Ref. 13, in which the relaxation time was determined from the pressure dependence of the duration of the PA signal compression pulse.

Relaxation of water vapor at excitation of the (100–001) vibrational states was studied in Refs. 3–5, and the rate constants were estimated for the following transitions: (100–001)→(020), (020)→(010), and (010)→(000). The rate constants obtained in different papers have, naturally, somewhat different values. Table 2 presents relaxation rate constants[3–5] (along with the corresponding relaxation time at the pressure of 1 Torr) of the lowest vibrational state (010), since just its relaxation time forms the basis for model calculations presented below. Note that Ref. 3 studied relaxation of the $H_2{}^{18}O$ molecule, and for the (010) state the relaxation rate constant is spread in a rather wide range. It is for this reason that we used, in the estimates that follow, the mean value of this constant according to the data of Refs. 4 and 5, which is equal to 1.8 $\mu s^{-1} \cdot Torr^{-1}$.

Table 1. Rate constants and time of vibrational relaxation of the H_2O molecule as judged from experimental data[3–5,11–13]

Excited state	Buffer gas	Experimental data			Calculation	
		Rate (type) of elementary relaxation process k, in $\mu s^{-1} \cdot Torr^{-1}$	Relaxation time τ_{rel} at p = 1 Torr, in μs	Ref.	$\tau = 1/k$*, in μs	τ_Σ**, in μs
100, 001	H_2O	0.75 (100,001 → 020)		3	1.33	2.21
		3.0 (020 → 010)		($H_2{}^{18}O$)	0.33	
		1.8 (010 → 000)			0.56	
	O_2	0.011 (100,001 → 020)				
	N_2	0.015 (100,001 → 020)				
	H_2O	0.86 (100,001 → 020)		4	1.16	1.98
		3.96 (020 → 010)			0.25	
		1.77 (010 → 000)			0.56	
	H_2O	1.13 (100,001 → 020)		5	0.88	1.63
		4.5 (020 → 010)			0.22	
		1.9 (010 → 000)			0.53	
110, 011	H_2O	5.6		5		
103	H_2O		1.5	11		
			3.8			
	air		18			
			22			
	H_2O		3.8	12		
	air		70			
	H_2O		1.3	13		
	air		7.4			
	N_2		9.4			

* Calculated for elementary relaxation process, whose rate is given in this row.

** Calculated as the total time of sequential relaxation process τ_Σ (that is, the sum of τ values in the previous column).

Table 2. Relaxation rate of the lowest bending vibration $k(010 \rightarrow 000)$ obtained in Refs. 3–5 and the corresponding relaxation time (at p = 1 Torr)

$k(010 \rightarrow 000)$, $\mu s^{-1} \cdot Torr^{-1}$	$\tau(010)$, μs	Ref.
1.8 – 3.0	0.33 – 0.56	3
1.77 ± 0.27	0.49 – 0.67	4
1.9 ± 0.2	0.48 – 0.59	5

2. Population kinetics of H_2O vibrational states at selective pulsed excitation of high vibrational stretching mode

In the case of linear absorption of laser radiation by H_2O molecules, the change in population of vibrational states of a multilevel system is described by the system of equations

$$\frac{dN_i}{dt} = \sum_j k_{j,i} N_j + \kappa_i I(t) - \sum_j k_{i,j} N_i , \qquad (1)$$

where $I(t)$ is the intensity of the exciting radiation; κ is the absorption coefficient; $k_{j,i}$ is the rate of transition from the jth level to the ith level at collisions.

Formal solution of the system of kinetic equations (1) for populations of vibrational levels of gas molecules with allowance for all possible collisional transitions is rather complicated and includes a large number of parameters (rates and energy differences for all possible transitions), therefore it was assumed in calculation of the heat release rate for a multilevel gas that only the transitions to the lower-lying vibrational levels with $\Delta V = 1$ are allowed at collisions and the difference in the level energy leads to the increase in the kinetic energy of colliding molecules. Following this assumption, equations of the system (1) in sums include only the terms responsible for transitions from neighboring (and to neighboring) levels, and the population of the ith level is described by the sum, whose terms decrease exponentially with time and the rate of decrease is determined by the rate of relaxation of the levels having the energy higher than the ith level. For example, if the mth level is excited at absorption of a radiation pulse of the form $I(t) = \exp(-k_b t) - \exp(-k_f t)$, where k_f and k_b are the rates of increase and decrease of its leading and trailing edges, respectively, then the populations of the lower-lying levels are described by the equation

$$N_i(t) = A_f e^{-k_f t} + A_b e^{-k_b t} + \sum_{j=i}^{m} A_j e^{-k_{j,j-1} t} . \qquad (2)$$

The values of the coefficients A_f, A_b, and A_j are determined by the relation between the excitation and relaxation rates.

At excitation of high vibrational states, several levels may take part in the relaxation process. Relaxation of population of the ith level causes the heat release at a rate $h(\nu_i - \nu_{i-1}) k_{i,i-1} N_i$. Correspondingly, the total time for relaxation of the vibrational energy in a multilevel system is $\tau_\Sigma = \sum_i \frac{1}{k_{i,i-1}}$ and the total heat release rate equals $\sum_i h(\nu_i - \nu_{i-1}) k_{i,i-1} N_i$.

When constructing a model of the vibrational relaxation in the H_2O molecule, one should take into account the presence of three vibrational modes. We used the following assumptions:

1) according to the data of Refs. 3–5, stretching vibrational states relax via the closest neighboring bending level;

2) relaxation in a bending mode was estimated in the harmonic oscillator approximation according to Ref. 16;

3) the rate of vibrational relaxation for the transition (010)→(000) was taken equal to 1.8 $\mu s^{-1} \cdot Torr^{-1}$, and the range of variability of this parameter was specified as 1.5–2.1 $\mu s^{-1} \cdot Torr^{-1}$ in accordance with the experimental error in Refs. 4 and 5.

For illustration, Fig. 1 depicts the schematic of energy levels E_n of different vibrational states of the H_2O molecule with the energy up to 14800 cm^{-1} drawn according to data from Ref. 17. The lengths of bars in Fig. 1 are taken arbitrarily. Different lengths indicate that levels belong to different types of vibrational states.

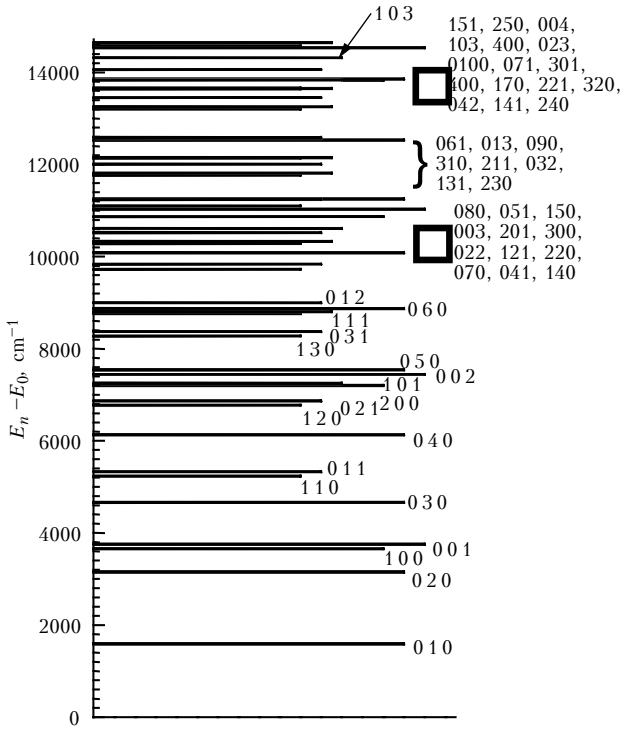

Fig. 1. Schematic of lower vibrational levels of the H_2O molecule. The vertical scale interval of 200 cm^{-1} is roughly equal to kT at 300 K.

3. Results and discussion

Within the harmonic oscillator model, the following is valid for the probability of transitions between neighboring vibrational levels[16]:

$$P(V + 1, V) \sim (V + 1).$$

This allows one to relate the relaxation rate of high vibrational states to the relaxation rate of the lower state as

$$k(0\ n\ 0 \rightarrow 0\ n - 1\ 0) = n\ k(010 \rightarrow 000). \qquad (3)$$

If anharmonism is taken into account, then Eq. (3) includes an additional factor, which, for example, for the 5 to 6-th vibrational level of the nitrogen molecule increases the probability of a single-quantum transition (and, correspondingly, the rate constant) by an order of magnitude.[18] However, when estimating the rates of transitions between bending levels of the H_2O molecule, we restricted our consideration to the harmonic oscillator model because no data concerning the effect of anharmonism on the probability of transitions in H_2O are available.

The transition rate constants for 10 lowest H_2O bending levels calculated using the experimental value of the relaxation rate for the lowest level (010) are given in the second column of Table 3. The rate values obtained for $k(010 \rightarrow 000) = 1.8\ \mu s^{-1}\cdot Torr^{-1}$ are given in bold, and the range of the possible rate values corresponding to $k(010 \rightarrow 000)$ ranging from 1.5 to $2.1\ \mu s^{-1}\cdot Torr^{-1}$ is given in parentheses. The third column gives the time for the corresponding transitions $\tau = 1/k$ at $p = 1$ Torr, and the fourth column presents the calculated total relaxation time at excitation of the corresponding level that was estimated as a sum duration of the sequential relaxation process involving transitions $(0\ n\ 0) \rightarrow (0\ n{-}1\ 0) \rightarrow \ldots \rightarrow (0\ 1\ 0) \rightarrow (000)$.

Table 3. Rate constants and the corresponding relaxation time (at $p = 1$ Torr) for 10 lowest bending levels

V_2	$k(V_2 \rightarrow V_2{-}1)$, $\mu s^{-1}\cdot Torr^{-1}$	$\tau(V_2 \rightarrow V_2{-}1)$, μs	τ_Σ, μs
1	**1.8** (1.5 – 2.1)	**0.56** (0.48 – 0.67)	**0.56** (0.48 – 0.67)
2	**3.6** (3.0 – 4.2)	**0.28** (0.24 – 0.33)	**0.83** (0.71 – 1.00)
3	**5.4** (4.5 – 6.3)	**0.19** (0.16 – 0.22)	**1.02** (0.87 – 1.22)
4	**7.2** (6.0 – 8.4)	**0.14** (0.12 – 0.17)	**1.16** (0.99 – 1.39)
5	**9.0** (7.5 – 10.5)	**0.11** (0.10 – 0.13)	**1.27** (1.09 – 1.52)
6	**10.8** (9.0 – 12.6)	**0.092** (0.079 – 0.111)	**1.36** (1.17 – 1.63)
7	**12.6** (10.5 – 14.7)	**0.079** (0.068 – 0.095)	**1.44** (1.23 – 1.73)
8	**14.4** (12.0 – 16.8)	**0.069** (0.060 – 0.083)	**1.51** (1.29 – 1.81)
9	**16.2** (13.5 – 18.9)	**0.062** (0.053 – 0.074)	**1.57** (1.35 – 1.89)
10	**18.0** (15.0 – 21.0)	**0.056** (0.048 – 0.067)	**1.63** (1.39 – 1.95)

Figure 2 depicts the relaxation time reduced to the pressure of 1 Torr as a function of the excitation energy. The solid line shows the calculated dependence of the relaxation time corresponding to the harmonic oscillator model. Experimental values are shown by symbols. In calculation it was assumed that $E_n - E_0 = n\,h\nu_2$.

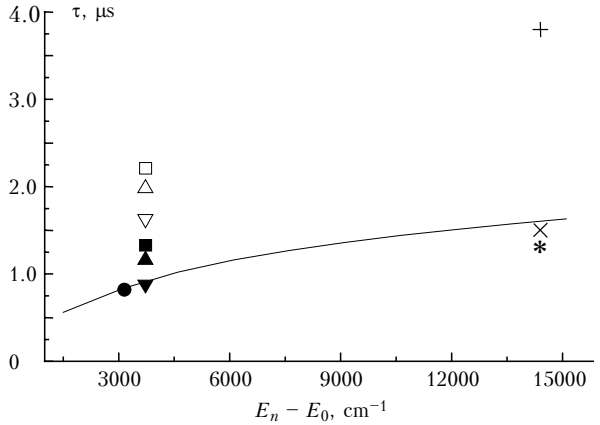

Fig. 2. Relaxation time for different H_2O vibrational levels at the pressure $p = 1$ Torr; calculation by the harmonic oscillator model (solid line); experimental data for $\tau(100,001 \rightarrow 020)$ (! 7 в), $\tau_\Sigma(\nu_1, \nu_3)$ (□ 8 x) (! and □ – from Ref. 3, 7 and 8 – from Ref. 4, в and x – from Ref. 5); $\tau_\Sigma(2\nu_2)$ (,), and $\tau_\Sigma(103)$ (× – from Ref. 11, + – from Refs. 11 and 12, ✻ – from Ref. 13).

Since in Refs. 3–5 there is no data on the relaxation time, closed symbols in Fig. 2 correspond to $\tau(\nu_1,\nu_3)$, and the open symbols are for τ_Σ calculated as described above. Note that the difference $\tau_\Sigma - \tau(\nu_1,\nu_3)$ corresponds to the relaxation time of the $2\nu_2$ level. The values of the relaxation time of the $2\nu_2$ level calculated based on the constants obtained in Refs. 3–5 appeared to be close, and these are shown by the same symbol (•) in Fig. 2. This symbol falls on the model curve. This coincidence can be considered as a confirmation of the applicability of the harmonic oscillator model to calculation of the rates of transitions between bending levels, at least, at not very large vibrational quantum numbers. It is also seen from Fig. 2 that the harmonic oscillator model is inapplicable to transitions between H_2O modes of different type.

To estimate the mean energy transferred into heat for a single collision at a high excitation energy of the molecule, we determined the mean time between two collisions using the mean values of collisional halfwidths γ_{col} of spectral lines based on the broadening coefficients taken from the HITRAN database[19] with the allowance for self-broadening and air pressure induced broadening. The obtained values of the time between collisions (and halfwidths used in their calculation) are given in Table 4.

Table 4. Mean energy transferred by the H_2O molecule for one collision at excitation of the (103) state

Buffer gas	Broadening coefficient, cm^{-1}/atm (Ref. 19)	γ_{col}, MHz (at $p = 1$ Torr)	$t_{col} = (2\pi\gamma_{col})^{-1}$, μs	ΔE, cm^{-1}
H_2O	0.44	17	0.009	100
air	0.087	3.4	0.046	90

The mean energy transferred was calculated as

$$\Delta E = (E_n - E_0)\ \frac{t_{col}}{\tau_{rel}},$$

where t_{col} is the time between collisions; the values of τ_{rel} at the excitation energy of 14400 cm^{-1} that were used in the calculations were taken from Ref. 13.

Using the values of the relaxation time from Table 1, we have calculated the mean energy ΔE transferred in a single collision at different excitation levels. The calculated results are summarized in Table 5. It should be noted that the values of ΔE are usually used as a characteristic of the relaxation process at high excitation energy, when it is difficult to speak about specific relaxation channels.[1,20–22] The values of ΔE calculated based on data from Refs. 3–5 on the relaxation are obviously inappropriate to this case, but we include them into Table 5 along with the ΔE values for relaxation of the (103) state[11–13] for a comparison. (As before, according to the results of Refs. 3–5, it was assumed that the vibrational (100, 001) states relax via energy transfer into the state (020), and then stepwise: (020) → (010) and (010) → (000), and the total relaxation time of the (100) and (001) states corresponds to τ_Σ from Table 1).

Table 5. Mean vibrational energy transferred in a single collision for the CS_2, SO_2 and H_2O molecules (cm^{-1}) at different excitation level

$E_n - E_0$, cm^{-1}	CS_2	SO_2	H_2O
500	–	2.2 (Ref. 6)	
1500	–	–	24 (Ref. 3)
			24 (Ref. 4)
			26 (Ref. 5)
2500	–	2.0 (Ref. 22)	–
3100	24 (Ref. 20)	–	32 (Ref. 3)
			34 (Ref. 4)
			37 (Ref. 5)
3700	–	–	15 (Ref. 3)
			17 (Ref. 4)
			20 (Ref. 5)
4600	37 (Ref. 20)	–	–
5000	37 (Ref. 21)	16 (Ref. 22)	–
9000	101 (Ref. 20)		–
10000	140 (Ref. 21)	120 (Ref. 22)	–
14400	–	–	34 (Refs. 11, 12)
			86 (Ref. 11)
			100 (Ref. 13)
20000	360 (Ref. 21)	600 (Ref. 22)	–
32600	650 (Ref. 20)	–	–
36000	490 (Ref. 21)	–	–
45600	–	840 (Ref. 22)	–

For a comparison, Table 5 presents also the mean energy transferred in a single collision between CS_2–CS_2 and SO_2–SO_2 (Refs. 20–22). The value of ΔE for SO_2 at the excitation energy ≈ 500 cm^{-1} was calculated from the collisional line halfwidth and the relaxation time of the lower vibrational level.[6] The closeness of this ΔE value to those obtained in Ref. 22 confirms the applicability of the calculation technique used. It is seen from Table 5 that at low excitation energy ~3500 cm^{-1} the mean energy transferred in H_2O–H_2O collisions ranges from 15 to 37 cm^{-1}, and as the excitation energy increases up to 14400 cm^{-1}, it increases up to 100 cm^{-1}. This fact is in qualitative agreement with the ΔE values for other molecules at the same excitation level.

The VT relaxation time obtained in Ref. 13 at excitation of the combination (103) state does not allow one to judge on the relaxation channels for vibrational energy, but this experimentally obtained value can be compared with the relaxation time values calculated using different models of energy transfer between levels with the rate constants from Tables 1 and 3. For analysis of possible channels of relaxation of the (103) state, let us consider some possible models of the relaxation process.

1. Assume that the (103) state relaxes by the same scheme as the (100–001) states do: the vibrational excitation is first transferred into a bending mode, and then stepwise relaxation by its levels occurs. It is seen from Fig. 1 that the energy levels of the H_2O molecule can be divided into several groups depending on their energy. In each group, the energy difference between neighboring levels is smaller than kT (~ 200 cm^{-1} at T = 300 K), therefore quick energy exchange without marked heat release is possible between these states. The groups are separated by the energy far exceeding kT, therefore transitions between levels from neighboring groups occur with lower probability and are accompanied by heat release. The level (103) and the state (0 10 0) of the bending mode are in the same energy group, therefore it would be expected that the first stage of relaxation takes short time, and the decisive factor is the time of energy transfer between levels of the bending mode τ_Σ. According to Table 3, for the level (0 10 0) it equals 1.63 μs at p = 1 Torr, which is somewhat higher than the value (1.3 ± 0.1) μs obtained experimentally in Ref. 13, but taking into account the error in the data from Refs. 4 and 5 the range of possible values of τ_Σ for (0 10 0) is 1.39–1.95 μs, which makes the agreement between the calculated and experimental values acceptable. Besides, it is seen from Fig. 1 that the (080) and (070) states are from the same group, and it can be assumed that the characteristic time of energy exchange between them is smaller than $\tau(080 \rightarrow 070)$ from Table 3, which equals 0.07 μs, and this decreases somewhat the time calculated by this model.

2. Also, it can be assumed that at H_2O–H_2O collisions the close-to-resonance intermolecular energy exchange $H_2O(V) + H_2O(0) \rightarrow H_2O(V-1) + H_2O(1)$ occurs, and the probability of this process is higher than the probability of VT relaxation $H_2O(V) + H_2O \rightarrow H_2O(V-1) + H_2O + \Delta E'$ (Ref. 16). If the probability of intermolecular resonance vibrational-vibrational (VV) exchange is close to unity, then, for example, energy transfer from the (0 10 0) state to the (010) state requires nine collisions, that is, it takes ~ 0.08 μs. Having added the relaxation time of the

(010) state obtained experimentally in Refs. 3–5, we obtain that the total time for relaxation of the (103) state is about 0.6 μs. It should be noted that thus calculated value can be considered only as the lower limit for the relaxation time of the (103) level, since the accurate data on the probability of intermolecular energy transfer are unavailable.

3. The VT relaxation via stretching mode levels is less probable because of the twice as large energy difference $\Delta E'$, but the resonance intermolecular exchange is possible in these modes as well, and in this case the energy is transferred from (103) to (100–001) for only three collisions, that is, the process takes about 0.03 μs. Then, according to Refs. 3–5, the energy is transferred into $2\nu_2$, from $2\nu_2$ into ν_2, and from ν_2 into the ground vibrational state. According to Refs. 4 and 5, these transitions take about 1.0, 0.24, and 0.54 μs, respectively, and therefore the entire energy transfer process will take about 1.8 μs. The value obtained falls within the range for the model 1 (VT relaxation via the closest bending vibration), but it is apparently greater than the experimental value (1.3 ± 0.1) μs. It should be noted that unlike the two previous models, in which the initial stages did not involve heat release at all, and the energy $\Delta E'$ transferred then into heat corresponded to the energy difference between neighboring levels of a bending mode (that is, remained almost the same), in the latter model the energy transferred into heat in the transition (100–001) → (020) is roughly thrice as small as that at the previous stages. Formation of a PA signal in this case may have some specific features, which, possibly, affect the measured value of the relaxation time.

Besides, the (103) state may relax not only by one of the considered channels, but also by several channels simultaneously as well, and therefore the experimentally observed time may have some intermediate value.

Figure 3 shows the calculated rate of heat release in the closed volume of a PA cell at the gas pressure of 1 Torr. In fact, it is a sort of a heat source arising in the cell volume due to relaxation. It is just this source that is responsible for appearance of the PA signal. The calculation was performed for three models of relaxation of the (103) state mentioned above.

1. First, vibrational energy transfer (103)→(0 10 0) for the short time without heat release, then stepwise relaxation from the state (0 10 0) into the unexcited state with transformation of the energy difference $\Delta E' = 1500$ cm^{-1} into the kinetic energy at each transition.

2. First, vibrational energy transfer (103)→(0 10 0) for the short time without heat release, then intermolecular exchange of vibrational energy at collisions $H_2O(0V_20) + H_2O(000) = H_2O(0\ V_2 - 1\ 0) + H_2O(010)$ without heat release, and then VT relaxation of the state (010).

3. Resonance transfer of vibrational energy by the levels of stretching modes to the states (100) and (001), then energy transfer into the bending mode (100–001) → (020) with $\Delta E' = 500$ cm^{-1} and relaxation in the bending mode with $\Delta E' = 1500$ cm^{-1}, at each transition.

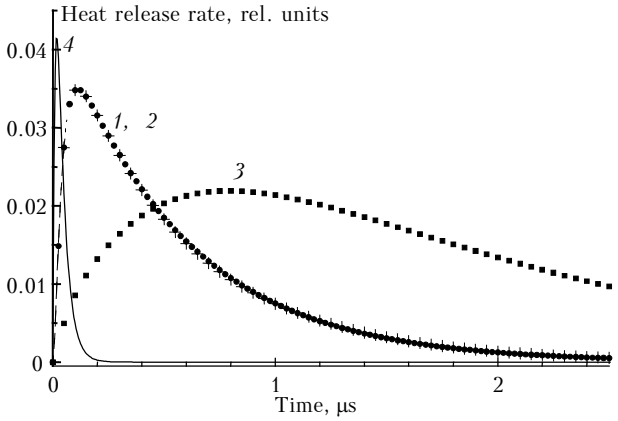

Fig. 3. Heat release signal in the PA cell: model 1 (+), model 2 (•), and model 3 (■); radiation pulse (solid curve).

The initial time of signal appearance in each model is quite conditional, since the duration of resonance vibrational transitions not accompanied by heat release can hardly be estimated. It is seen from Fig. 3 that the first two models are almost identical in the heat release rate, therefore they can hardly be distinguished in PA measurements, although they possibly have different time of beginning of the heat release. The heat release process corresponding to the third model differs considerably from the two previous ones in duration, namely, the duration of the heat release pulse (at half-maximum) for the third model is almost twice as long as those for the other two models.

The relaxation times at collisions of the H_2O molecule in air and nitrogen (the corresponding values are given in Table 1) were obtained in Ref. 13 along with the relaxation time at excitation of the vibrational (103) state in pure water vapor. This allowed us to estimate the relaxation time at collisions with oxygen, which appeared to be 4.0 μs·Torr if air is assumed to be a mixture of 80% nitrogen and 20% oxygen.

Although no one of the considered models of relaxation yielded the calculated relaxation time at excitation of the (103) state that would be close to the experimental value (1.3 μs·Torr for H_2O–H_2O collisions), the discrepancy between calculation and experiment for the first and third models is ~ 23 and 40%, respectively, and the minimum relaxation time estimated by the second model actually does not exceed the experimental value. The closest agreement between the calculation by the first model and the experiment confirms the fact that the most probable relaxation channel is relaxation via the closest level of the bending mode, as was already observed in Refs. 3–5 at excitation of the (100–001) states.

In measurements of the relaxation time in mixtures of water vapor with nitrogen and with air, the H_2O/buffer gas pressure ratio was 1:15. Since under such conditions the probability of resonance

intermolecular VV exchange at collisions is low, we used the model 1 in analysis of experimental values of the relaxation time at collisions of H_2O molecules with nitrogen or oxygen molecules. The rate constants of the transitions $k(010 \rightarrow 000)$ obtained in this case were 0.73 $\mu s^{-1} \cdot Torr^{-1}$ and 0.31 $\mu s^{-1} \cdot Torr^{-1}$ at collisions of H_2O with O_2 and N_2, respectively, that is 2.5 and 6 times smaller than at H_2O–H_2O collisions.

Conclusion

Based on the analysis performed, we have estimated the relaxation rate constants for bending mode levels and the mean energy transferred in a single collision for the H_2O molecule. The obtained mean energy transferred in a single collision for the water molecule as a function of the energy of exciting radiation is in qualitative agreement with the data of other investigators[1,20–22] for the triatomic CS_2 and SO_2 molecules, which differ by the structure, mass, dipole moment, etc.

The relaxation rate constant for the $2\nu_2$ level given in Table 3 corresponds to the data from Refs. 4 and 5 with the allowance made for the error. Unfortunately, experimental data on the relaxation of higher levels of the bending mode are unavailable, therefore there are no other direct confirmations for the obtained rates of transitions between the levels of bending mode of the water molecule. The agreement between the relaxation time measured experimentally and calculated by the harmonic oscillator model at excitation of the (103) vibration in the H_2O molecule indirectly confirms the applicability of the harmonic oscillator model to description of the rates of transitions between bending mode levels and the validity of the rate constants presented in Table 3.

However, it should be emphasized that the information available is insufficient for revealing the dominant relaxation channel at excitation of the combination (103) vibration. Besides, the relaxation rate of the (110–011) vibration obtained in Ref. 5 and equal to 5.6 $\mu s^{-1} \cdot Torr^{-1}$ is indicative of the quick energy exchange of the group of (110–011) levels with others, although it is accompanied by a significant heat release ($\Delta E' \approx 600$ cm^{-1}). Therefore, there is, possibly, one more energy transfer channel that fell beyond the scope of this paper.

Acknowledgments

The authors are thankful to Dr. B.A. Tikhomirov for experimental data on relaxation of the (103) vibration of the H_2O molecule kindly presented at their disposal, as well as for useful criticism and discussion of the results obtained.

Support from the Russian Foundation for Basic Research (Project No. 00–05–65082) is acknowledged.

References

1. R.G. Hynes and M.G. Sceats, J. Chem. Phys. **91**, No. 11, 6804–6812 (1989).
2. M. Capitelli, ed., *Nonequilibrium Vibrational Kinetics* (Springer-Verlag, 1986).
3. J. Finzi, F.E. Hovis, V.N. Panfilov, P. Hess, and C.B. Moore, J. Chem. Phys. **67**, No. 9, 4053–4061 (1977).
4. P.F. Zittel and D.E. Masturzo, J. Chem. Phys. **90**, No. 2, 977–989 (1989).
5. P.F. Zittel and D.E. Masturzo, J. Chem. Phys. **95**, No. 11, 8005–8012 (1991).
6. P.V. Slobodskaya and E.N. Rityn', Opt. Spektrosk. **47**, No. 6, 1066–1072 (1979).
7. F. Menard-Bourcin, L. Doyennette, and J. Menard, J. Chem. Phys. **92**, No. 7, 4212–4221 (1990).
8. F. Menard-Bourcin, J. Menard, and L. Doyennette, J. Chem. Phys. **94**, No. 3, 1875–1881 (1991).
9. V. Zeninari, B.A. Tikhomirov, Yu. N. Ponomarev, and D. Courtois, J. Chem. Phys. **112**, No. 4, 1835–1843 (2000).
10. A.D. Bykov, L.N. Sinitsa, and V.I. Starikov, *Experimental and Theoretical Methods in Molecular Spectroscopy of Water Vapor* (SB RAS Publishing House, Novosibirsk, 1999), 376 pp.
11. V.A. Kapitanov, O.Yu. Nikiforova, Yu.N. Ponomarev, and B.A. Tikhomirov, Atmos. Oceanic Opt. **7**, Nos. 11–12, 790–794 (1994).
12. V.A. Kapitanov and B.A. Tikhomirov, Appl. Opt. **34**, No. 6, 969–972 (1995).
13. B.A. Tikhomirov and A.B. Tikhomirov, in: *Abstracts of 12th CPPP* (Toronto, 2002), No. 266.
14. A.B. Antipov, V.A. Kapitanov, Yu.N. Ponomarev, and V.A. Sapozhnikova, *Photoacoustic Method in Laser Spectroscopy of Molecular Gases* (Nauka, Novosibirsk, 1984), 128 pp.
15. Yu.N. Ponomarev, B.G. Ageev, M.W. Sigrist, V.A. Kapitanov, D. Courtois, and O.Yu. Nikiforova, *Laser Photoacoustic Spectroscopy of Intermolecular Interactions in Gases*, ed. by L.N. Sinitsa (RASKO, Tomsk, 2000), 200 pp.
16. V.N. Kondrat'ev and E.E. Nikitin, *Kinetics and Mechanism of Gas-Phase Reactions* (Nauka, Moscow, 1974), 560 pp.
17. H. Partridge and D.W. Schwenke, J. Chem. Phys. **106**, No. 11, 4618–4639 (1997).
18. E.E. Nikitin, *Theory of Elementary Atomic-Molecular Processes in Gases* (Khimiya, Moscow, 1970), 456 pp.
19. L.S. Rothman, C.P. Rinsland, A. Goldman, S.T. Massie, D.P. Edwards, J.-M. Flaud, A. Perrin, C. Camy-Peyret, V. Dana, J.-Y. Mandin, J. Schroeder, A. McCann, R.R. Gamache, R.B. Wattson, K. Yoshino, K.V. Chance, K.W. Jucks, L.R. Brown, V. Nemtchinov, and P. Varanasi, J. Quant. Spectrosc. Radiat. Transfer **60**, No. 6, 665–710 (1998).
20. J.E. Dove, H. Hippler, and J. Troe, J. Chem. Phys. **82**, No. 4, 1907–1919 (1985).
21. M. Heymann, H. Hippler, H.J. Plach, and J. Troe, J. Chem. Phys. **87**, No. 7, 3867–3874 (1987).
22. M. Heymann, H. Hippler, D. Nahr, H.J. Plach, and J. Troe, J. Phys. Chem. **92**, No. 19, 5507–5514 (1988).